

A CONSERVATIVE COUPLING NUMERICAL METHOD FOR TRANSIENT CONJUGATE HEAT TRANSFER

Emmanuel Radenac*, Jérémie Gressier*, Pierre Millan* and André Giovannini†

*French National Aerospace Research Establishment (ONERA)
2 avenue Edouard Belin - BP 4025, 31055 Toulouse Cedex 4, France
e-mail: emmanuel.radenac@oncert.fr, web page: <http://www.onera.fr>

†Toulouse Fluid Mechanics Institute (IMFT)
1 allée du Professeur Camille Soula, 31400 Toulouse, France
Web page: <http://www.imft.fr>

Key words: Heat transfer, Fluid Mechanics, Coupling boundary conditions, Finite Volume method, Conservativity, Stability analysis

Abstract. *A conservative fluid mechanics-heat diffusion solver coupling method is presented. Optimal use of solvers can be achieved by coupling according to a cycle time step independent of classical numerical stability conditions. Solvers integrate their domains independently during a cycle. Between cycles, data are exchanged to compute a coupling boundary condition, which is imposed at the interface between the coupled domains. Conservativity is one of the main purposes of this coupling method. Consequently, Finite Volume method is used for the solvers. But during independent integrations by solvers, thermal flux losses happen at the interfaces between coupled domains. Conservative corrections are defined and used in order to maintain conservativity. But they can destabilize time integration. Stability criteria are established in order to achieve a robust conservative coupling, that eventually also improves integration accuracy.*

1 INTRODUCTION

The study of fluid-solid conjugate heat transfer is essential for technologies that involve a lot of aerothermal phenomena. They result from interactions between flows and solids with very different temperatures, complex thermal boundary conditions and geometries. Consequently, aeronautical industries (including spatial ones) are interested in a better knowledge of conjugate heat transfer. There is a particular need in the fields of jet engines and in transient studies.

Analytical results are not numerous and limited to very simple geometries (such as forced convection over an infinite or semi-infinite thick flat plate^{1,2} or in a channel with

b	thermal effusivity	λ	thermal conductivity
E	thermal energy	τ	diffusion characteristic time
F	Fourier number	$\vec{\cdot}$	vector
h	convection coefficient	$\hat{=}$	2D matrix
k	conservative correction coefficient	\cdot	perturbation
r	thermal effusivity ratio		
S	surface	Subscripts:	
T	temperature	b	boundary
t	time	c	cycle
x	1D spatial coordinate	e	external condition
α	thermal diffusivity	i	interface
χ	diffusion characteristic time ratio	L	left zone
$\vec{\Phi} = -\lambda \vec{\nabla} T$	thermal flux	R	right zone

Table 1: Nomenclature

thick walls³). So, numerical simulations of the coupled fluid-solid phenomena are essential. For a long time, they used to consist in decoupled studies: for instance, numerical flow simulations were made with given thermal boundary conditions (often adiabatic or isothermal). But these imposed boundary conditions were not satisfactory: the flow creates convection that modifies the temperature in the solid. In order to perform an accurate integration of flow and solid, it is necessary to calculate the right boundary condition at the interface of these fluid and solid domains.

To date, many studies have been already led, giving mainly steady results for turbine aerothermic fields^{4,5,6,7}. Few data can be found for unsteady simulations^{8,9}. However, for instance in the case of a jet engine, many transient phases occur during a flight. The example of the high speed flight phase, that is usually short, shows the importance of a best knowledge of transient phenomena. Knowing precisely the maximum temperature reached by materials during this short phase could allow to reduce the safety margins usually set by steady-state results.

2 CONJUGATE HEAT TRANSFER

To integrate simultaneously a solid and a fluid, a good numerical solution is to use solvers which are well adapted to the domains to be calculated: a fluid mechanics Navier-Stokes one for the fluid and a thermal diffusion one for the solid. Coupling these solvers consists in imposing a proper thermal boundary condition at the common boundary of the solid and fluid domains.

The usual thermal boundary conditions are the following ones (notations of figure 1):

- Dirichlet (or isothermal) boundary condition: temperature is imposed at the boundary: $T_b = T_e$.
- Neumann boundary condition: thermal flux is imposed at the boundary: $\Phi_b = \Phi_e$.

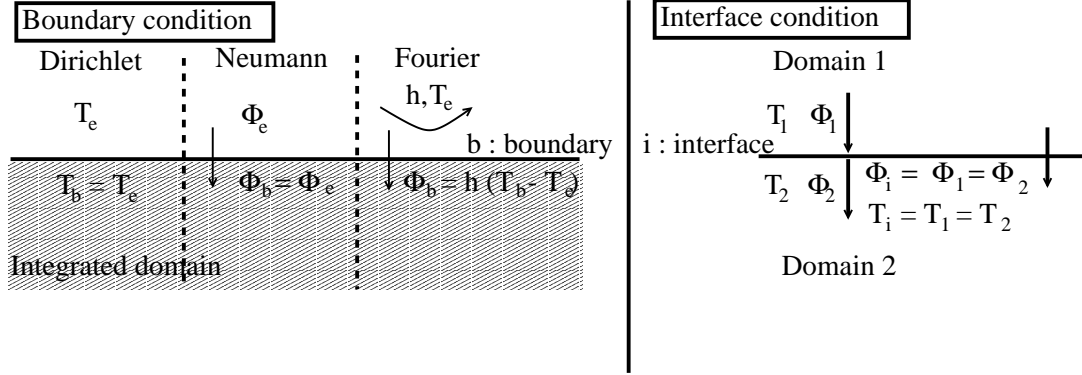


Figure 1: Thermal boundary and interface conditions

If Φ_e is zero, the boundary condition is adiabatic.

- Fourier (or convection) boundary condition: a linear relation between interface thermal flux and temperature is imposed, thanks to a convection coefficient h and a fluid temperature T_e :

$$\Phi_b = h(T_b - T_e) \quad (1)$$

At the interface between two domains (figure 1), fluid or solid, the physical condition is conservation of thermal flux and temperature (with the hypothesis of perfect thermal contact):

$$\begin{aligned} \Phi_i &= \Phi_1 = \Phi_2 \\ T_i &= T_1 = T_2 \end{aligned} \quad (2)$$

Eventually, the coupling strategy is to divide the whole field in solid and fluid domains. These zones are integrated by proper solvers. The boundary conditions at the domain interfaces ensure conservation of both flux and temperature through the interface.

3 OVERVIEW OF COUPLING METHODS

The coupling method is also defined by the coupling process: the chronology of domain integration and interface boundary condition calculation. The actual nature of interface boundary conditions is also a crucial choice.

3.1 Coupling process

The coupling process can be sequential or parallel. Subsequently, coupling will systematically involve left (L) and right (R) domains respectively integrated by solvers L and R .

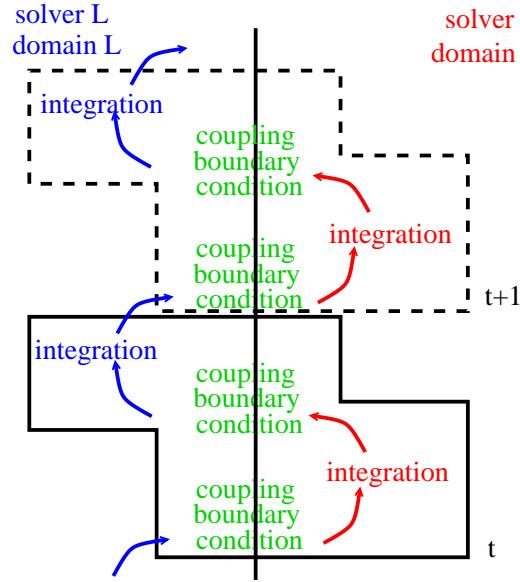


Figure 2: Coupling sequential process

In a sequential process (figure 2), each domain is integrated one after the other and gives its thermal boundary condition as coupling boundary condition for the other domain at the cycle completion. This coupling method is used by Sondak and Dorney⁸ and Rahaim *et al*⁹ for their unsteady solver couplings.

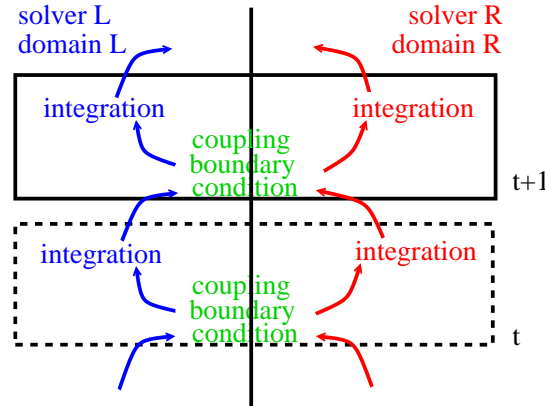


Figure 3: Coupling parallel process

In a parallel process (figure 3), used for instance by Montenay *et al*⁶, both domains are calculated simultaneously. At the end of both integrations, a coupling boundary condition is calculated and is used as boundary condition for both domains during following cycle. Simultaneous temporal integration fits better the unsteadiness constraint. Moreover, the sequential process generally does not allow an instantaneous conservation of both interface

temperature and thermal flux. This balance is obtained only at convergence to steady state.

As a consequence, the parallel process is chosen for the unsteady coupling described in this article.

3.2 Coupling boundary conditions

Many authors (such as Thakur *et al*⁷) chose the couple of boundary conditions at the interface between fluid and solid domains as follows: the fluid gives its thermal flux to the solid and the latter gives its temperature to the former. So the fluid domain receives a Dirichlet boundary condition and the solid domain a Neumann one. This choice, that seems natural to thermics specialists, is also justified by stability analyses such as Giles' one¹⁰.

Neumann boundary condition is sometimes changed into a Fourier one in order to improve stability of the coupling process⁶.

Both these choices of boundary condition couples are not intended to conserve instantaneously interface temperature and thermal flux. Once again, the balance is only obtained at convergence to steady state. For an unsteady process, it is better to impose this conservation at each coupling iteration. Some authors¹¹ manage to get it by use of a single Navier-Stokes code, that integrates the solid parts with the energy equation only. The whole field is obtained with the same solver and interface conditions are given by the internal scheme. Conservation of flux and temperature is obtained naturally.

In the coupling method described here after, the coupling boundary conditions can be Dirichlet, Fourier or Neumann ones but are calculated in order to conserve simultaneously and instantaneously temperature and flux, according to the integration scheme.

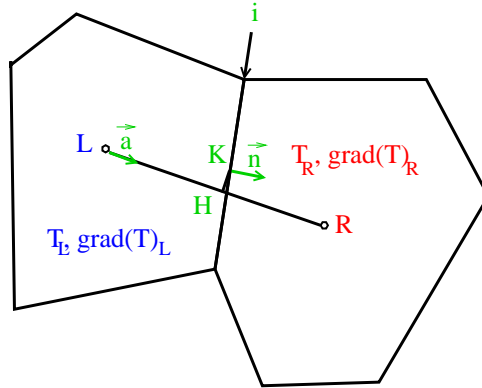


Figure 4: Adjacent cells neighboring a coupling interface

The selected discretization method of both solvers is Finite Volume method. In the case of matching meshes, the configuration of interface and adjacent cells is showed on figure 4. L , R and K are respectively the left and right cell and interface centers. Interface

temperature T_i and thermal flux Φ_i are conserved together if: $\Phi_i = \Phi_L = \Phi_R$, with figure 4 notations:

$$\begin{aligned}\Phi_L &= -\lambda_L \frac{T_K - T_L}{\|\vec{L}\vec{K}\|} \frac{\vec{L}\vec{K} \cdot \vec{n}}{\|\vec{L}\vec{K}\|} = -\lambda_L \frac{T_K - T_L}{d_L} \\ -\Phi_R &= -\lambda_R \frac{T_K - T_R}{\|\vec{R}\vec{K}\|} \frac{\vec{R}\vec{K} \cdot \vec{n}}{\|\vec{R}\vec{K}\|} = -\lambda_R \frac{T_K - T_R}{d_R}\end{aligned}\quad (3)$$

Interface temperature is inferred from T_K :

$$T_i = \frac{\frac{\lambda_L}{d_L} T_L + \frac{\lambda_R}{d_R} T_R}{\frac{\lambda_L}{d_L} + \frac{\lambda_R}{d_R}} \quad (4)$$

with:

$$d_L = \frac{\vec{L}\vec{K} \cdot \vec{L}\vec{K}}{|\vec{L}\vec{K} \cdot \vec{n}|} \quad \text{and} \quad d_R = \frac{\vec{R}\vec{K} \cdot \vec{R}\vec{K}}{|\vec{R}\vec{K} \cdot \vec{n}|} \quad (5)$$

Eventually, interface thermal flux is given by inserting T_i in relation 3:

$$\Phi_i = \frac{2\lambda_L\lambda_R}{d_L d_R \left(\frac{\lambda_L}{d_L} + \frac{\lambda_R}{d_R} \right)} (T_R - T_L) \quad (6)$$

A Dirichlet condition is set with T_i , a Neumann condition with Φ_i and a Fourier condition for instance in the left domain with $h = \frac{\lambda_R}{d_R}$ and $T_e = T_R$.

4 COUPLING PROCESS

The chosen coupling process is parallel. Domain time integrations are made in parallel and a coupling procedure makes them exchange data in order to update the coupling boundary conditions.

4.1 Strict process

In a strict coupling process, the coupling procedure would be called at each integration time step (figure 5). In this case, everything happens as if the whole domain was a single one: the solid and fluid domains always depend on each other during the time integration. This process is the one used when a single Navier-Stokes solver integrates the whole domain, taking into account the energy equation only for solids. But it implies a common time step, given by the smallest one, for all domains. However, integration time steps are usually given by stability criteria that may result in very different time discretizations according to the domain. This process is not optimal.

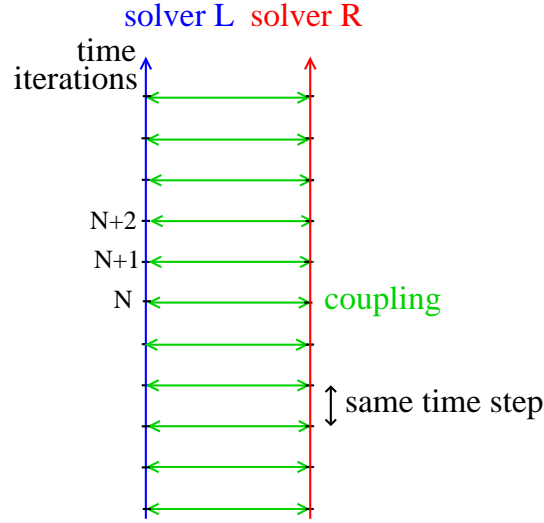


Figure 5: Strict coupling process

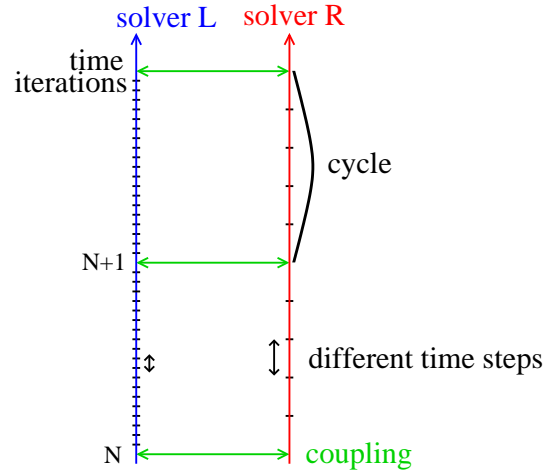


Figure 6: Cycle-based coupling process

4.2 Cycle-based coupling

In order to allow different domain time discretizations, cycles are defined (figure 6). Their duration is independent of usual stability conditions and set by the user according to physical criteria for example. The coupling procedure is called at the beginning of each cycle: coupling boundary conditions are updated and remain the same all cycle long. The domains are then integrated independently during the cycle.

This coupling process makes communications between domains sparse, making parallelization easy.

With strict process, as the domain integrations are never independent, all kinds of

coupling boundary conditions are equivalent. They simply conserve interface flux and temperature by different algorithmic ways. In cycle-based coupling, when different zones are integrated independently with given coupling boundary conditions, the nature of these ones is crucial. For instance, if the boundary conditions are Neumann ones, interface flux is set for the whole cycle. It ensures there are no flux losses during the cycle. But interface temperature changes according to this flux condition and to domain temperature repartition. Its conservation during the cycle is not ensured at all. There is also the danger that this temperature increases far too much, especially in cases where two domains of initial different temperatures are coupled. At the right beginning, the thermal flux are large and can lead to high interface temperatures for long cycles. If the coupling boundary conditions are Dirichlet ones, interface temperature is balanced all cycle long and there is no danger of temperature evolution to very high levels. But interface flux conservation is not allowed. Eventually, with Fourier conditions, neither interface thermal flux nor temperature are balanced during the cycle.

5 CONSERVATIVITY

One of the coupling method main purposes is conservativity, which prevents flux losses due to discretization.

5.1 Choice of the solvers

Intrinsically conservative Finite Volume method is used for both fluid mechanics and heat diffusion solvers. Conservativity in each integrated zone is ensured thanks to this discretization method. But at domain interfaces, especially with cycle-based coupling, conservation of thermal flux is not so easy.

5.2 Necessity of conservative corrections

As explained before, independent domain integrations during cycles can lead to flux losses (if one of the coupling boundary conditions is not a Neumann one). A simple example shows the necessity of a conservative coupling procedure: two 1D solid walls of initial different temperatures (1000 K in the left one, 500 in the right one), with a common face and adiabatic conditions at the extremities (figure 7). These boundary conditions are particularly severe for conservativity: if all boundaries are adiabatic, there must be no thermal flux losses. Theoretical result is a uniform 700K temperature in the whole field. Table 2 sums up relative errors on final temperature obtained for different cycle length (given by the non dimensional parameter cycle Fourier number: $F_c = \frac{\alpha \delta t_c}{\delta x^2}$ where δt_c is the cycle time step, common to both domains, α the material thermal diffusivity, different according to the domain, and δx^2 the spatial discretization). The coupling boundary conditions are isothermal ones. Flux losses lead to a wrong final temperature and the relative error can be large for long cycles.

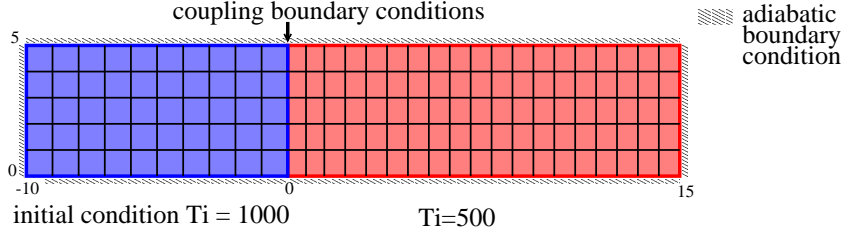


Figure 7: Example of adiabatic case meshing for conservative coupling validation

CYCLE FOURIER NUMBERS (L/R)	RELATIVE ERROR
10/5.2	13.7%
20/10.4	18.8%
40/20.8	22.9%
160/83.3	27%

Table 2: Relative error on final temperature for non conservative coupling with cycles of increasing length

5.3 Conservative correction method

In order to correct interface flux losses, a correction method with following strategy is used:

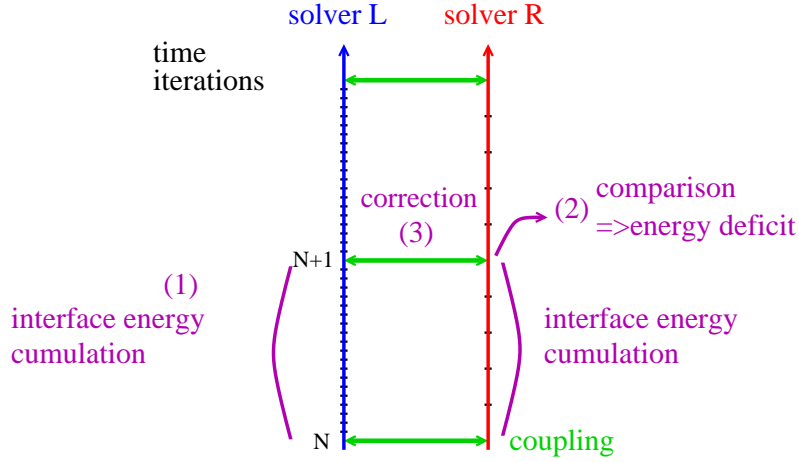


Figure 8: Correction method

1. computation of losses: interface thermal flux are cumulated during the cycle in all domains (figure 8). It results for each zone in a thermal energy crossing the interface $E = \int_{t_N}^{t_{N+1}} \int_S \vec{\Phi}(t) \cdot d\vec{S} dt$. At the end of the cycle, during the coupling procedure, at a given interface, the energies obtained for both zones are compared.
2. estimation of conservative correction: as there is an energy deficit, an estimation of the physical right amount must be imposed arbitrarily. A correction coefficient k

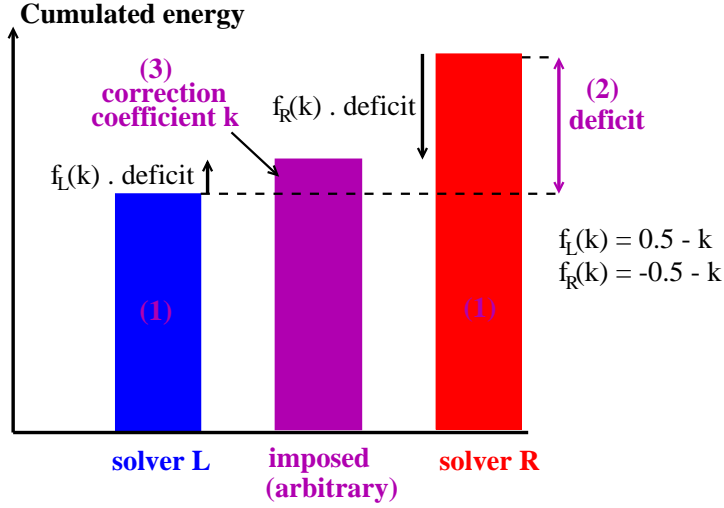


Figure 9: Correction method: estimation of the corrective energy increment

balances the estimation between the energies obtained in both domains (figure 9). k takes values between -0.5 and 0.5 , and defines a spatial correction distribution. For instance, for $k = +0.5$, the estimated interface energy will be left (L) domain's one and the right (R) domain receives correction.

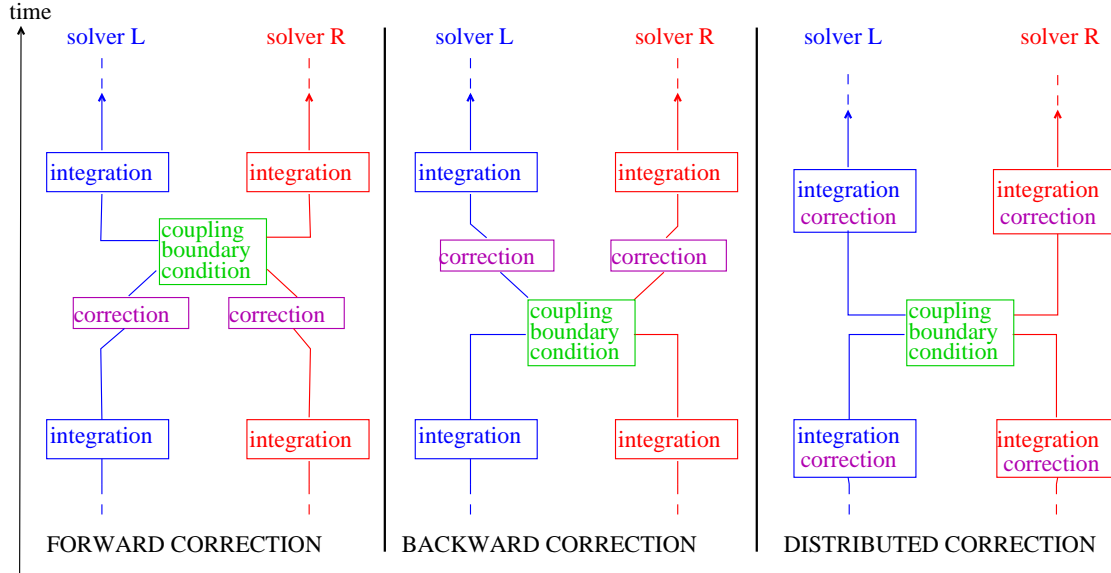


Figure 10: Conservative correction time distribution

- application of correction: the corrective energy ΔE , obtained after cumulation and spatial distribution thanks to k , is applied as a corrective temperature increment

ΔT in the adjacent cells:

$$\Delta T = \frac{\Delta E}{\rho c_P} \quad (7)$$

A time distribution is made too (figure 10): the correction can be applied before updating coupling boundary conditions or after (respectively **forward** and **backward** corrections). It can even be distributed over a given number of integration iterations of the following cycle (**distributed** correction).

5.4 Main parameters

These corrections allow a conservative coupling method. The stability and precision of the method are studied subsequently. There are two kinds of parameters for this study:

- two physical parameters, that are the classical ratios (for two coupled zones L and R) for thermally coupled fluid-solid phenomena, the ones found in analytical studies:

1. the coupled domain diffusion characteristic time ratio $\chi = \frac{\alpha_R \delta x_L^2}{\alpha_L \delta x_R^2} = \frac{\tau_L}{\tau_R}$
2. the coupled domain effusivity ratio $r = \frac{b_R}{b_L}$

- three user parameters, still to be defined by stability and accuracy analyses:

1. the coupling boundary conditions couple
2. the conservative correction spatial distribution: the correction coefficient k
3. the conservative correction time distribution

6 CORRECTIONS AND STABILITY

The coupling method is expected to be robust: a stability analysis will specify the user parameters to use in order the coupling to be stable.

6.1 A destabilization due to corrections

It is observed that the conservative correction method destabilizes time integration.

Without corrections, couplings with boundary condition couples involving Fourier or Dirichlet conditions are stable. The stability analysis assumes cycles long enough to obtain steady state in every domain at every cycle. These long cycles are not suitable for unsteady applications but they are a critical condition for coupling. Indeed, the longer is the cycle, the more the evolution of temperature in the different domains can lead to uncorrect temperature distributions. This stability analysis proves that, with at least one Neumann coupling boundary condition (that is to say a Neumann condition for one

domain and a Dirichlet, Fourier or Neumann condition for the other one), stability is very dependent on spatial discretization. With refined meshes, the coupling may not be very robust. On the contrary, the other kinds of coupling boundary conditions are stable.

Consequently, only the choices Dirichlet/Dirichlet (Dirichlet condition for both domains), Dirichlet/Fourier and Fourier/Fourier can be safely used for coupling.

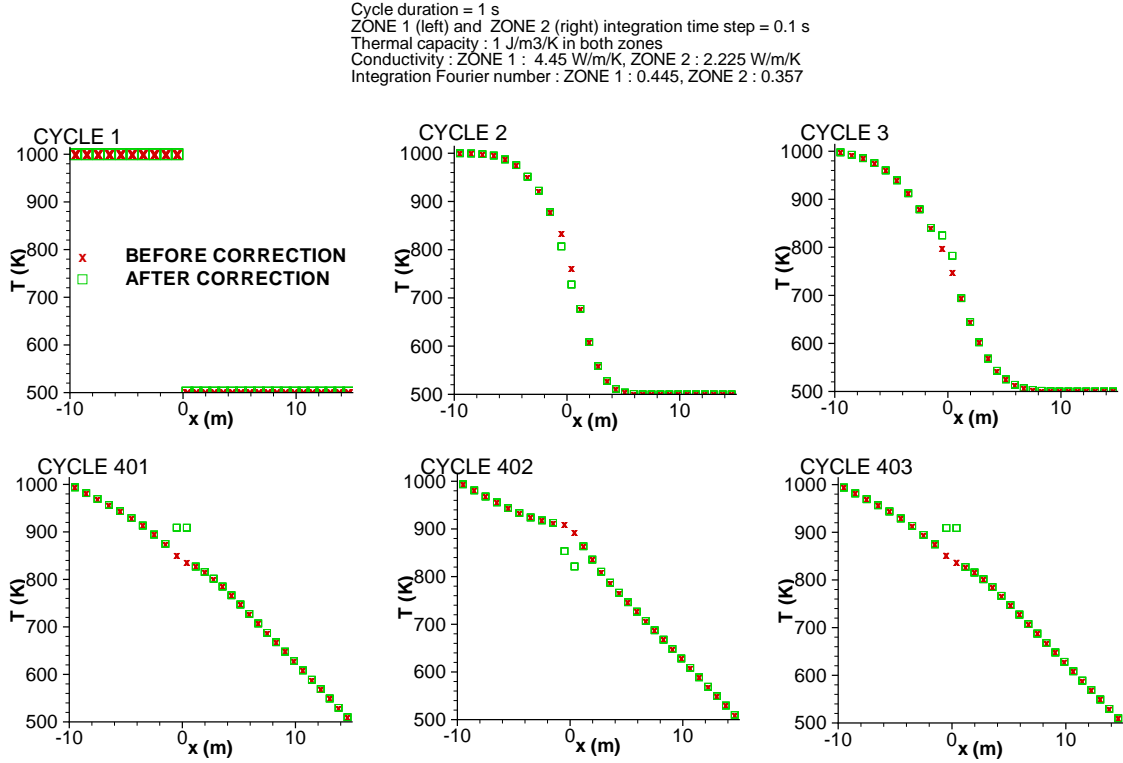


Figure 11: Destabilization due to corrections

However, using, for example, a Dirichlet/Dirichlet couple, an integration with conservative corrections can be unstable (figure 11). The corrective temperature increment amplifies cycle after cycle because correction is too large. A stability analysis decoupling totally correction process from domain integrations proves that it is intrinsically destabilizing. Cycles can stabilize integration thanks to diffusion of the corrective temperature increment. A global stability analysis quantifies the stability in terms of maximum cycle Fourier number. It allows to specify user parameters according to physical coupling parameters.

6.2 Global stability analysis

The whole algorithm has been implemented to achieve a stability analysis of small perturbations, based on the Matrix Method¹² (that can provide information on the influence

of boundary conditions). Error amplification during a cycle with conservative corrections is studied. The analysis, based on the coupling of two finite 1D walls with isothermal conditions at the extremities, is described in Appendix. Length of both walls is given by cell numbers. The results given with 10 or 20 cells do not show any variation. The influence of the interface phenomena is primordial.

For this type of theoretical analysis, only **forward** and **backward** corrections can be evaluated.

The results are given as a function of χ and r . These ratios are defined as the right wall thermal property over the left wall one: $\chi = \frac{\alpha_R \delta x_L^2}{\alpha_L \delta x_R^2} = \frac{\tau_L}{\tau_R}$ and $r = \frac{b_R}{b_L}$. χ takes values between 0 and 1: cases $\chi > 1$ are inferred from the wall coupling symmetry. Stability is qualified in terms of maximum cycle Fourier numbers, computed in the left wall.

6.3 Results

For a large range of ratios χ and r and for three different correction coefficients, the maximum cycle Fourier number is computed for the three types of boundary condition couples involving Dirichlet and Fourier conditions. The tested correction coefficients impose a correction applied totally in a domain ($k = -0.5$ and 0.5 respectively in the left and right one) or in two equal parts in both domains ($k = 0$).

Figure 12 shows, in the plan (χ, r) , for different values of k , the best couple for **forward** correction, that is the one giving the highest allowable cycle Fourier number. These maximum cycle Fourier numbers are showed by figure 13.

First observation is that, whatever r , the maximum cycle Fourier number are much higher with $k = +0.5$. As $\chi \leq 1$, a first crucial conclusion is that the correction has to be applied preferentially in the domain where the diffusion characteristic time is the highest. Moreover, the coupling seems all the more stable as χ is small. Two explanations are combined. First, the temperature evolutions being slower, the state at the end of the cycle is further from convergence to steady state. A too large corrective increment diffuses less and the consequences are smaller. Second, a small α can be due to a large ρc_P . In this case, the corrective temperature increment is smaller (equation 7).

Figure 13 shows that the Dirichlet/Fourier boundary condition pair is preferable (especially in case $k = +0.5$ that gives the best cycle Fourier numbers when $\chi \leq 1$). More precisely, the Fourier condition has to be imposed in the domain where correction is applied.

This stability analysis allows to choose the coupling boundary condition pair and the conservative correction spatial distribution. Its time distribution remains to be chosen.

With **backward** correction, which is a first step towards a distribution of correction over the following cycle, stability can not be defined in terms of maximum cycle Fourier number any longer. But criterium is integration Fourier number (based on integration time step instead of cycle duration). Figure 14 shows that, whatever k and the number of iterations per cycle, stability is ensured for a large range of r and χ , for integration

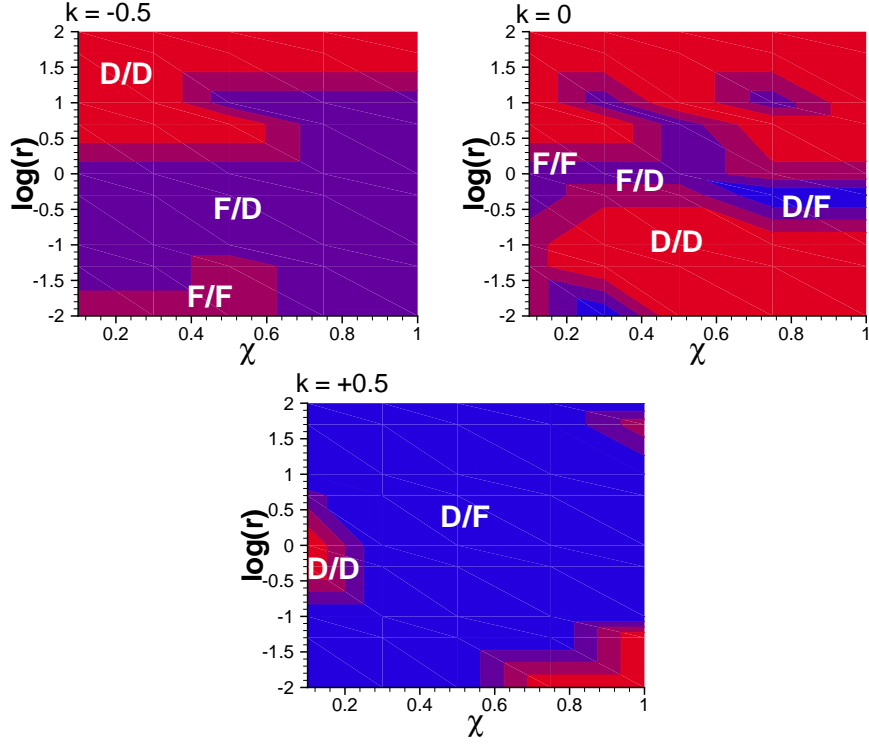


Figure 12: Best coupling boundary condition couples C_L/C_R ($C = D$: Dirichlet condition, $C = F$: Fourier condition), according to physical coupling parameters and correction coefficient

Fourier numbers less than 0.4. A maximum cycle Fourier number would be given by the product of the maximum integration Fourier number and the number of iterations per cycle. However, as the maximum integration Fourier number is the same for every number of iterations per cycle (until 500), no cycle Fourier number criterium can be defined and the cycle Fourier numbers reach very high values. Eventually, moving the correction after the updating of coupling boundary conditions improves stability.

Unluckily, stability analysis results are rather sensitive to mesh quality and multiple zones coupling. Numerical experiments are made with non-uniform meshes and couplings involving many zones so that some cells could receive corrections from many interfaces (figure 15). Especially in the second kind of configuration, the stability criteria obtained theoretically prove to be underestimated. But distributing the corrective increment over the cycle is a good solution that allows to restore robustness.

7 Accuracy

As it could be expected with adiabatic results, integration accuracy is improved by the conservative coupling method. As the coupling method is based on interface heat diffusion, theoretical studies can be led with multi-material cases instead of fluid-solid cases.

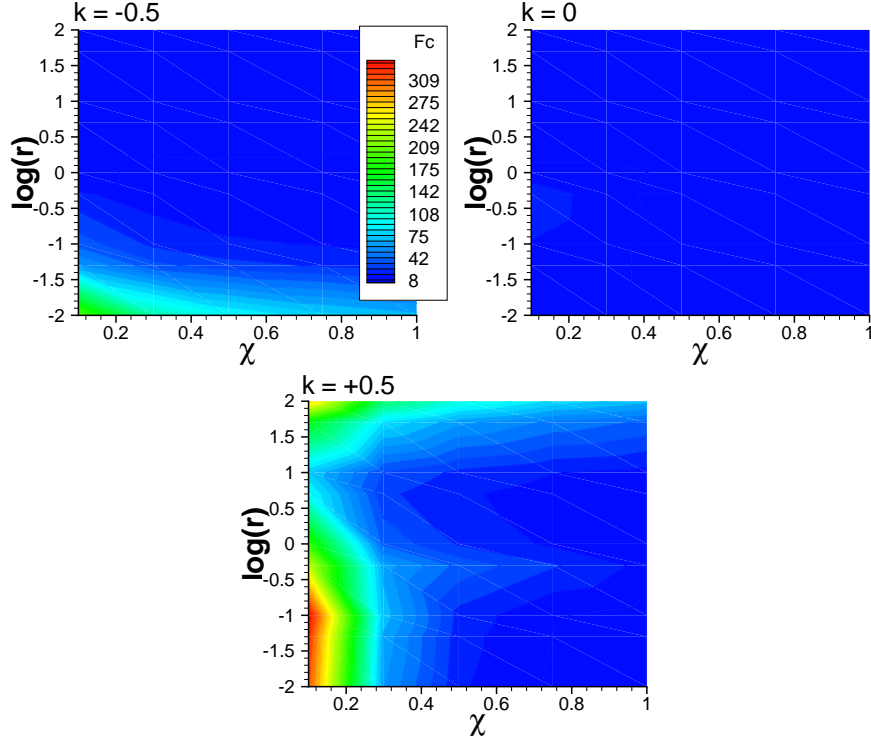


Figure 13: Maximum cycle Fourier number obtained with best coupling boundary condition couple according to physical coupling parameters and correction coefficient

A simple example of wall coupling, with different convection conditions at the extremities (figure 16) shows the accuracy improvement. Initial temperatures in both walls are different: there is immediately an interface thermal flux and conservative corrections are necessary at once. Cycles are rather long: $\delta t_c = 50s$ (diffusion characteristic times, based on wall thickness, are $666s$ and $4500s$ respectively for the left and right walls). Integration Fourier number being 0.3 , there are respectively 50 and 22 iterations per cycle for the left and right walls. Conservative corrections are the most stable: $\chi = 0.5$ imply correction in the right domain and that coupling boundary conditions are Dirichlet in the left domain and Fourier in the right one.

On figure 17, comparison of numerical results of interface temperature with analytical results shows good agreement for different conservative methods and a rather large error for not conservative coupling. At initial times, all methods give a rather large relative error. Finite Volume method imposes an interface temperature (equation 4) different from theoretical result at $t = 0s$:

$$T_i = \frac{b_L T_L + b_R T_R}{b_L + b_R} \quad (8)$$

Initial intrinsic error is not improved when there are interface thermal flux losses. The three kinds of conservative correction time distribution improve accuracy with little

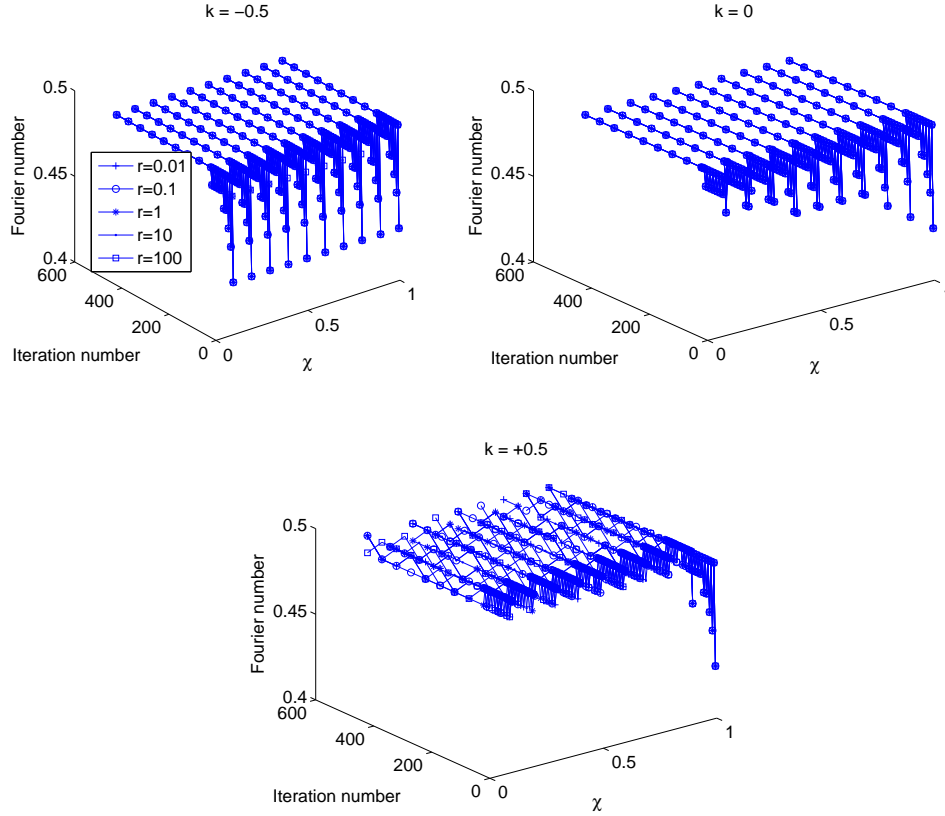


Figure 14: **backward** correction. Maximum integration Fourier number obtained with Dirichlet/Dirichlet coupling boundary condition couple according to physical coupling parameters and correction coefficient

difference. **forward** correction is a bit better than the other ones. Unlike the other, it allows coupling boundary conditions to depend on corrected temperatures immediately. But it is less stable: interface temperature oscillations can be observed for small times. They prefigure destabilization.

8 CONCLUSION

A robust, accurate, conservative coupling method for transient conjugate heat transfer has been proposed. A Navier-Stokes and a heat diffusion solver can be coupled with a user-defined coupling time discretization that control communication between solvers. The period during which solvers function independently is called a cycle.

Instantaneous conservation of domain interface temperature and thermal flux is ensured by well-chosen coupling boundary conditions. These boundary conditions allow parallel independent domain integrations by solvers during cycles.

Conservativity is obtained through the use of Finite Volume method and of a correc-

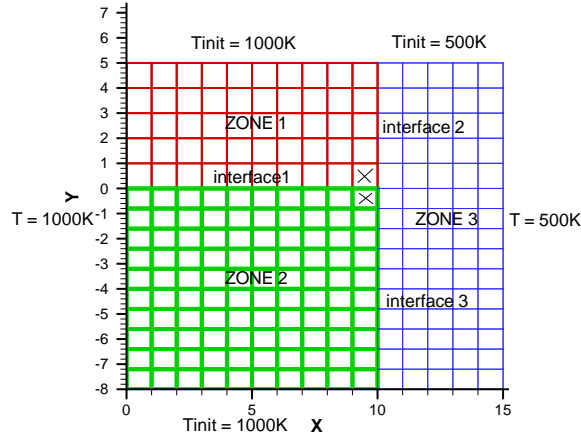


Figure 15: Correction critical case mesh: the two marked cells can get corrections from two interfaces

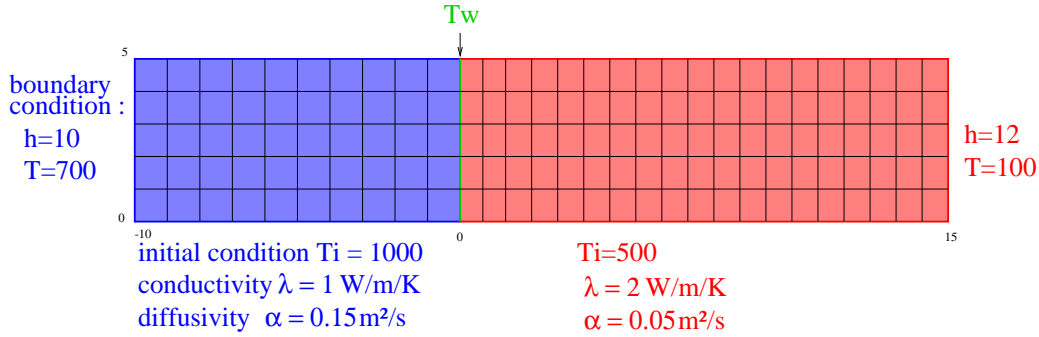


Figure 16: Accuracy validation case

tion method that compensates interface thermal flux losses due to independent domain integrations during cycles. The conservative correction method destabilizes integration. Its spatial and time distribution as well as coupling boundary conditions nature are set so that the coupling remains stable.

Conservative correction also improves integration unsteady accuracy, as shown by a basic example.

APPENDIX

The stability analysis of conservative coupling is based on the Matrix Method. Two coupled zones are discretized in n_L and n_R cells respectively (figure 18) and a coupling boundary condition stocking cell per zone is added (n'_L and n'_R). Boundary conditions at the extremities are isothermal.

Both zones have the same time discretization and there are N time steps per cycle.

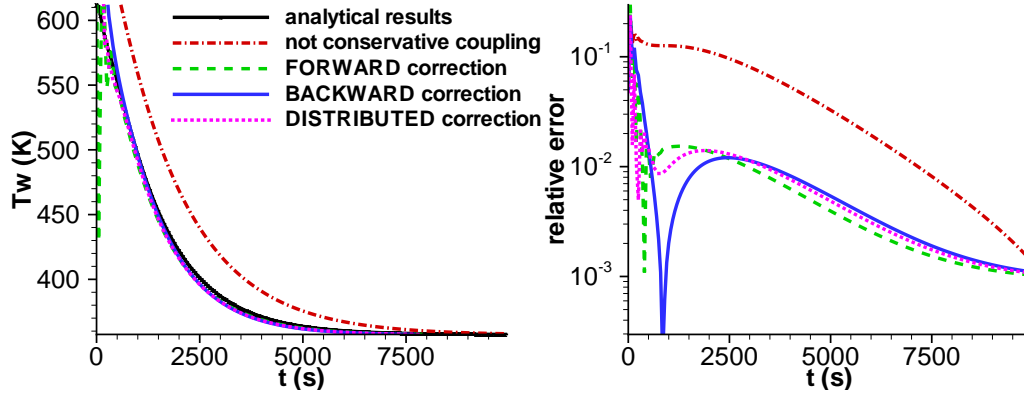


Figure 17: Conservative coupling method accuracy validation

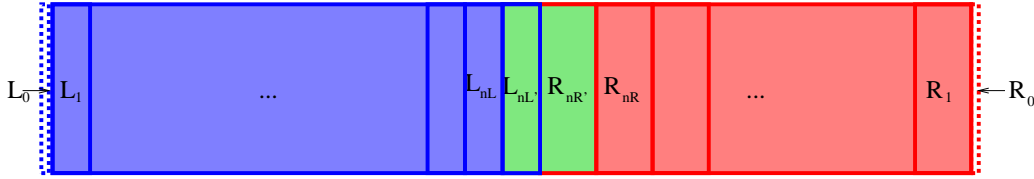


Figure 18: Conservative coupling method stability analysis mesh

These N iterations are followed by two pseudo iterations, N' and N'' that are necessary for taking into account correction and coupling boundary conditions computation.

A temperature perturbation is written at each point i of this mesh and at each iteration n : $\tilde{T}_i^n = T_i^n + \delta T_i^n$. The purpose of the analysis is to write the perturbation vector $\underline{\delta T}$ at iteration N'' (end of the cycle) as a function of its initial value ($n = 0$: beginning of the cycle): $\underline{\delta T}^{N''} = \underline{C}_{N''} \underline{\delta T}^0$. The perturbation vector is:

$$\underline{\delta T}_L^n = \begin{pmatrix} \delta T_{L_1}^n \\ \vdots \\ \delta T_{L_{nL}}^n \\ \delta T_{L_{nL'}}^n \end{pmatrix}, \underline{\delta T}_R^n = \begin{pmatrix} \delta T_{R_{nR'}}^n \\ \delta T_{R_{nR}}^n \\ \vdots \\ \delta T_{R_1}^n \end{pmatrix} \Rightarrow \underline{\delta T}^n = \begin{pmatrix} \underline{\delta T}_L^n \\ \underline{\delta T}_R^n \end{pmatrix}$$

$\underline{C}_{N''}$ is the cycle amplification matrix. Stability is conditional to a spectral radius of this matrix lower than 1. $\underline{C}_{N''}$ depends on three distinct actions:

1. Separate cycle integration for n from 0 to $N - 1$, $J = L$ or R (explicit scheme):

$$\begin{aligned} i \in \{2, \dots, nJ - 1\} \text{ (internal cell): } & \delta T_{J_i}^{n+1} = (1 - 2F_J)\delta T_{J_i}^n + F_J\delta T_{J_{i+1}}^n + F_J\delta T_{J_{i-1}}^n \\ i = 1 \text{ (isothermal condition): } & \delta T_{J_1}^{n+1} = (1 - 3F_J)\delta T_{J_1}^n + F_J\delta T_{J_2}^n \\ i = nJ: & \text{dependent on coupling condition} \\ i = nJ' \text{ (stocking cell): } & \delta T_{J_i}^{n+1} = \delta T_{J_i}^n \end{aligned}$$

2. Correction pseudo-iteration ($n = N'$ for **forward** correction, $n = N''$ for **backward** correction):

$$i \in \{1, \dots, nJ - 1\} \cup \{nJ'\}: \delta T_{J_i}^n = \delta T_{J_i}^{n-1}$$

$$i = nJ: \delta T_{J_i}^n = \delta T_{J_i}^{n-1} - k_J \delta C_J \text{ with:}$$

$$k_J = \begin{cases} k - 0.5 & \text{if } J = L \\ -k - 0.5 & \text{if } J = R \end{cases}$$

δC_J is the perturbed corrective temperature increment in domain J , dependent on the coupling boundary conditions.

3. Coupling boundary condition computation pseudo-iteration ($n = N''$ for **forward** correction, $n = N'$ for **backward** correction):

$$i \in \{1, \dots, nJ\}: \delta T_{J_i}^n = \delta T_{J_i}^{n-1} \text{ (internal cells)}$$

$$i = nJ': \text{ dependent on coupling condition}$$

Eventually, with $\underline{\underline{M_I}}$, $\underline{\underline{M_C}}$ and $\underline{\underline{M_{BC}}}$ respectively the independent cycle integration, conservative correction and coupling boundary condition computation matrices, the cycle amplification matrix is:

$$\underline{\underline{C_{N''}}} = \begin{cases} \underline{\underline{M_{BC}}} \left(\underline{\underline{M_I}}^N + \underline{\underline{M_C}} \sum_{n=0}^{N-1} \underline{\underline{M_I}}^n \right) & \text{forward correction} \\ \underline{\underline{M_{BC}}} \underline{\underline{M_I}}^N + \underline{\underline{M_C}} \sum_{n=0}^{N-1} \underline{\underline{M_I}}^n & \text{backward correction} \end{cases}$$

REFERENCES

- [1] A. Pozzi, R. Tognaccini and A. Della Rocca. Coupling of convection and conduction in the fluid with conduction in the solid: spatial and temporal singularities. *16th AIMETA Congress of Theoretical and Applied Mechanics*, (2003).
- [2] C. Treviño, A. Espinoza and F. Mendez. Asymptotic analysis of the transient conjugate heat transfer process between two forced counterflowing streams. *SIAM J. Appl. Math.*, **vol. 57 No. 3**, 577-596, (1997).
- [3] B. Fourcher and K. Mansouri. An approximate analytical solution to the Graetz problem with periodic inlet temperature. *Int. J. Heat and Fluid Flow*, **vol. 18**, 229-235, (1997).
- [4] D. V. Roscoe, A. K. Tolpadi and R. C. Buggeln. Numerical analysis of conjugate heat transfer and fluid flow in disk pumping applications. *AIAA Paper*, **92-0397**, (1992).

- [5] K.-H. Kao and M.-S. Liou. Application of chimera/unstructured hybrid grids for conjugate heat transfer. *AIAA Journal*, **vol. 35 No. 9**, 1472-1478, (1997).
- [6] A. Montenay, L. Paté and J.-M. Duboué. Conjugate heat transfer analysis of an engine internal cavity. *ASME Paper 2000, GT282*, (2000).
- [7] S. Thakur and J. Wright. Conjugate heat transfer in a gas turbine blade trailing-edge cavity. *AIAA Paper*, **2002-0496**, (2002).
- [8] D. L. Sondak and D. J. Dorney. Simulation of coupled unsteady flow and heat conduction in turbine stage. *Journal of Propulsion and Power*, **vol. 16 No. 6**, (2000).
- [9] C. P. Rahaim, A. J. Kassab and R. J. Cavalleri. Coupled dual reciprocity boundary element/finite volume method for transient conjugate heat transfer. *Journal of thermophysics and heat transfer*, **vol. 14 No. 1**, 27-38, (2000).
- [10] M. B. Giles. Stability analysis of numerical interface conditions in fluid-structure thermal analysis. *International Journal of Numerical Methods in Fluids*, (1997).
- [11] D. Bohn, H. Schönenborn, B. Bonhoff and H. Wilhelmi. Prediction of the film-cooling effectiveness in gas turbine blades using a numerical model for the coupled simulation of fluid flow and diabatic walls. *ISABE*, **95-7105**, (1995).
- [12] C. Hirsch. *Numerical computation of internal and external flows*, John Wiley and Sons, Vol. I., (1988).

